The EMBO Journal Vol.17 No.9 pp.2687–2698, 1998

RAD9 and *RAD24* define two additive, interacting branches of the DNA damage checkpoint pathway in budding yeast normally required for Rad53 modification and activation

Maria-Angeles de la Torre-Ruiz, Catherine M.Green and Noel F.Lowndes[1]

Imperial Cancer Research Fund, Clare Hall Laboratories, CDC Laboratory, South Mimms, Herts EN6 3LD, UK

[1]Corresponding author
e-mail: lowndes@icrf.icnet.uk

In budding yeast, *RAD9* and *RAD24/RAD17/MEC3* are believed to function upstream of *MEC1* and *RAD53* in signalling the presence of DNA damage. Deletion of any one of these genes reduces the normal G_1/S and G_2/M checkpoint delays after UV irradiation, whereas in *rad9*Δ–*rad24*Δ cells the G_1/S checkpoint is undetectable, although there is a residual G_2/M checkpoint. We have shown previously that *RAD9* also controls the transcriptional induction of a DNA damage regulon (DDR). We now report that efficient DDR induction requires all the above-mentioned checkpoint genes. Residual induction of the DDR after UV irradiation observed in all single mutants is not detectable in *rad9*Δ–*rad24*Δ. We have examined the G_2/M checkpoint and UV sensitivity of single mutants after overexpression of the checkpoint proteins. This analysis indicates that *RAD9* and the *RAD24* epistasis group can be placed onto two separate, additive branches that converge on *MEC1* and *RAD53*. Furthermore, *MEC3* appears to function downstream of *RAD24/RAD17*. The transcriptional response to DNA damage revealed unexpected and specific antagonism between *RAD9* and *RAD24*. Further support for genetic interaction between *RAD9* and *RAD24* comes from study of the modification and activation of Rad53 after damage. Evidence for bypass of *RAD53* function under some conditions is also presented.

Keywords: budding yeast/checkpoints/DNA damage/repair/transcription

Introduction

Cells have evolved multiple strategies for tolerating genomic damage. The most important of these are numerous repair systems that remove or bypass potentially mutagenic DNA lesions (Friedberg *et al*., 1995). However, other cellular responses to DNA lesions are also important for the maintenance of genome stability. Delays at multiple cell-cycle transitions have long been recognized after exposure of both mammalian and yeast cells to DNA-damaging agents (Burns, 1956; Brunborg and Williamson, 1978; Murnane, 1995). The genetic control of these delays, termed 'checkpoints', was first established in budding yeast by Weinert and Hartwell (1988) who showed that the *RAD9* gene functions in G_2/M arrest after irradiation with X-rays. Subsequently, it has become clear that *RAD9* also functions at the G_1/S (Siede *et al*., 1993, 1994), intra-S (Paulovich *et al*., 1997) and mid-anaphase (Yang *et al*., 1997) checkpoints. Defects in checkpoint regulation can lead to genome instability and, in higher eukaryotes, neoplastic transformation (Hartwell and Kastan, 1994; Morgan and Kastan, 1997).

Genetic analysis in the budding yeast has identified a further six genes, *RAD17*, *RAD24*, *RAD53*, *MEC1*, *MEC3* and *DDC1*, in addition to *RAD9*, that appear to be required for efficient DNA damage-dependent checkpoints at G_1/S, intra-S and G_2/M (Elledge, 1996; Longhese *et al*., 1997). Of these genes, *RAD53* and *MEC1* are also required for an S/M checkpoint in which the presence of unreplicated DNA prevents the onset of mitosis (Elledge, 1996). Preliminary evidence for the order of function for this DNA structure checkpoint pathway(s) has come from analysis of the radiation-sensitive phenotype of certain mutants. Thus, *RAD9* is in an epistasis group distinct from *RAD24*, and *RAD17*, *MEC3* and *DDC1* are members of the *RAD24* epistasis group (Eckardt Schupp *et al*., 1987; Lydall and Weinert, 1995; Longhese *et al*., 1997). The position of *MEC1* relative to *RAD9* and the *RAD24* epistasis group is, however, not clear from these analyses. *RAD53* is believed to function further downstream, as the Rad53 protein is phosphorylated after DNA damage in a *MEC1*-dependent manner (Sanchez *et al*., 1996) and overexpression of *RAD53* can bypass deficiencies in *RAD9* and *MEC1* (Allen *et al*., 1994; Sanchez *et al*., 1996).

DNA damage in *Saccharomyces cerevisiae* results in a rapid transcriptional response (Friedberg *et al*., 1995). Recently, we described a role for *RAD9* in this transcriptional response leading to the induction of a large regulon of >15 genes with roles in DNA repair (Aboussekhra *et al*., 1996). The observation that this DNA damage regulon (DDR) is genetically and co-ordinately controlled in a *RAD9*-dependent manner is reminiscent of the SOS response of *Escherichia coli* where a regulon of similar genes with roles in DNA repair is also induced rapidly after DNA damage (Walker, 1984; Shinagawa, 1996). Interestingly, the *MEC1* and *RAD53* genes are themselves in the DDR (Aboussekhra *et al*., 1996; Kiser and Weinert, 1996), suggesting a degree of positive feedback regulation in this pathway.

Here we demonstrate that single mutants in either *RAD9* or the *RAD24* epistasis group are not completely defective for checkpoint activity in either G_1/S or G_2/M, whereas in the *rad9*Δ–*rad24*Δ double mutant the G_1/S checkpoint is not detectable and there is only a residual G_2/M checkpoint. This indicates that *RAD9* and *RAD24* control the majority of the DNA damage checkpoint capacity in *S.cerevisiae*. We have used overexpression analysis to demonstrate that *RAD9* and the *RAD24* epistasis group are partially redundant in function, operate upstream of

RAD53, as expected, and also of *MEC1*. This analysis also suggests an order of function within the *RAD24* epistasis group. Furthermore, we extend our previous observations on the *RAD9*-controlled DNA damage-dependent transcriptional response by showing that *RAD9*, *RAD24*, *RAD17*, *MEC3*, *MEC1* and *RAD53* are equally important for induction of the DDR. The residual transcriptional induction observed in single mutants is not observed in a *rad9*Δ–*rad24*Δ double mutant. Thus *RAD9* and the *RAD24* epistasis group contribute additively and equivalently to both checkpoint delays and the transcriptional response after DNA damage. Overexpression studies also demonstrate a specific and reciprocal antagonism between *RAD9* and *RAD24*. Support for this data suggesting genetic interaction between *RAD9* and *RAD24* comes from study of the phosphorylation of Rad53. The phosphorylation and activation of Rad53 kinase is dependent on both *RAD9* and the *RAD24* epistasis group but, under some circumstances, the checkpoint pathway can function in the absence of active Rad53 kinase. Together, our data indicate that the efficient functioning of two upstream branches, defined by *RAD9* and *RAD24*, of the DNA damage checkpoint pathway is required for a fully integrated response to DNA damage.

Results

The rad9Δ–rad24Δ double mutant abolishes the G_1/S checkpoint and virtually all of the G_2/M checkpoint after UV damage

We have shown previously that *rad9*Δ cells are not completely defective in the G_2/M checkpoint (Aboussekhra *et al*., 1996), suggesting a *RAD9*-independent contribution. We considered the possibility that both *RAD9* and the *RAD24* epistasis group would be required for fully functional checkpoints, both in G_1/S and in G_2/M. We examined the G_1/S checkpoint after UV irradiation in wild-type, *rad9*Δ, *rad24*Δ and *rad9*Δ–*rad24*Δ cells by monitoring the appearance of budded cells after release from a G_1 block (Figure 1A). The appearance of budded cells indicates the release of cells from the G_1 block into the cell cycle. Similarly to previous reports (Siede and Friedberg, 1990; Siede *et al*., 1993, 1994; Longhese *et al*., 1996), resumption of the cell cycle after release from the α-factor block in irradiated wild-type cells was significantly delayed by 30–40 min compared with the non-irradiated control. This delay in appearance of budded cells as a response to UV treatment was reduced to ~20 min in both *rad9*Δ and *rad24*Δ single mutants. In contrast, the *rad24*Δ–*rad9*Δ double mutant showed no detectable G_1/S delay after UV irradiation; rather the kinetics of appearance of budded cells was not significantly different from that of unirradiated wild-type cells, indicating that the G_1/S checkpoint is not detectable in these cells.

To support these data, we performed a second set of experiments that examined the G_2/M checkpoint (Figure 1B). Exponentially growing wild-type, *rad9*Δ, *rad24*Δ and *rad9*Δ–*rad24*Δ cells were UV irradiated and the proportion of G_2 cells monitored. The UV-irradiated culture of wild-type cells displayed a marked G_2/M checkpoint, producing a maximum of 50% G_2/M-blocked cells after 3 h. Interestingly, by monitoring the proportion of unbudded or small budded cells under these conditions, we have never

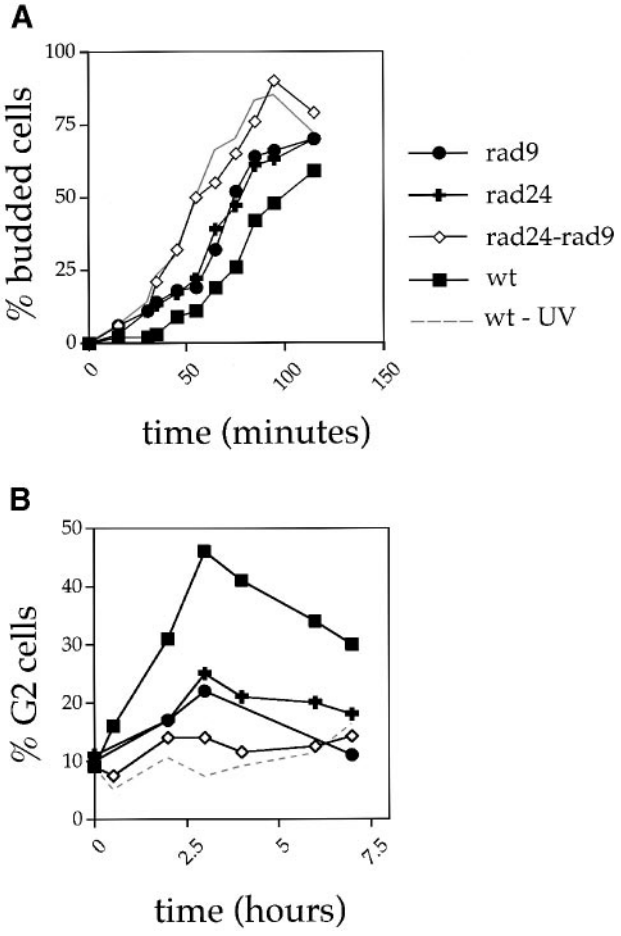

Fig. 1. G_1/S and G_2/M checkpoints after UV irradiation in wild-type, *rad9*Δ, *rad24*Δ and *rad9*Δ–*rad24*Δ cells. (**A**) Exponentially growing haploid cells were blocked in G_1 with α-factor, UV irradiated (45 J/m^2) and then released from the α-factor block into fresh, pre-warmed YNB plus 2% glucose. The percentage of budded cells was calculated 0, 15, 30, 35, 45, 55, 65, 75, 85, 95 and 115 min after the release and then plotted versus time. (**B**) Exponentially growing haploid cells were UV irradiated (45 J/m^2), resuspended in fresh pre-warmed YNB plus 2% glucose and the percentage of cells in G_2 were calculated as the number of large budded cells with single nuclei (DAPI stained) in the bud neck, and plotted versus time. Error bars were avoided in order to simplify the figure, but standard deviations from at least three experiments were <2.5% in all cases.

observed evidence for a significant G_1/S checkpoint (data not shown), indicating the dominance of the G_2/M checkpoint. In agreement with our previous observations (Aboussekhra *et al*., 1996), a residual G_2/M cell cycle delay was observed for *rad9*Δ cells, corresponding in this experiment to ~20% G_2/M cells after 3 h. A similar G_2/M delay was observed in *rad24*Δ (Figure 1B). However, the residual G_2/M checkpoint delay apparent in single null mutants of *RAD9* or *RAD24* is reduced further in *rad9*Δ–*rad24*Δ cells. Similarly, we have demonstrated a residual G_2/M checkpoint in single mutants, which reduced still further in the double mutant, by monitoring the delayed release from a nocodazole block after UV irradiation (data not shown).

We have demonstrated that *rad9*Δ–*rad24*Δ cells are more defective in their G_1/S and G_2/M checkpoints than the respective single mutants. These data suggest a model that places *RAD9* and *RAD24* on separate but additive

branches of the DNA damage-dependent checkpoint pathway. To confirm this model further, we also examined *mec3*Δ and *rad9*Δ–*mec3*Δ cells for their radiation sensitivity and G_1/S and G_2/M checkpoints. We observed that these phenotypes were more defective in *rad9*Δ–*mec3*Δ cells than in either *rad9*Δ or *mec3*Δ single mutants (data not shown). *rad9*Δ–*mec3*Δ cells, however, showed less marked phenotypes than the *rad24*Δ–*rad9*Δ cells, indicating that a strictly linear pathway within the *RAD24* epistasis group is unlikely.

RAD24, RAD17, MEC3, MEC1 and RAD53 have equivalent roles to RAD9 in regulation of the transcription response to DNA damage

RAD9 is required for the transcriptional induction of the DDR after DNA damage (Aboussekhra *et al*., 1996). We therefore investigated the role of the *RAD24* epistasis group in the regulation of the DDR; *MEC1* and *RAD53* were also tested for this response. Exponentially growing *rad9*Δ, *rad24*Δ, *rad17*Δ, *mec3*Δ and *mec1-1* cells were arrested in G_1 with α-factor, and either irradiated or mock irradiated while maintaining the G_1 arrest. This protocol allows damage-specific transcriptional induction to be examined in the absence of cell-cycle regulation and outside of S phase. We examined transcription of several genes representing different functional groups within the DDR: *CDC9* (DNA ligase); *DUN1* and *RAD53* (protein kinases involved in cellular responses to DNA damage); *RAD51* (a *recA* homologue); and *RNR1* (a large subunit of ribonucleotide reductase). *RNR3* was also probed with qualitatively similar results (data not shown). A clear defect in the transcriptional response of all the genes tested was observed in *rad9*Δ, *rad24*Δ, *rad17*Δ, *mec3*Δ and *mec1-1* mutants compared with the wild-type strain (Figure 2A). We also observed similar transcriptional defects using the *sad1-1* mutant allele of *RAD53* constructed in the W303 background (data not shown, but for the *RNR1* transcript see also Figure 4D). The transcriptional induction defect was similar among all of the mutants. The highest absolute levels of induction detected in wild-type cells were with the *RNR1*, *RNR3* (data not shown) and *RAD51* transcripts (Figure 2B). Although the absolute levels of induction observed in the wild-type for the other inducible genes tested, *CDC9*, *DUN1* and *RAD53*, were less dramatic, the dependency on an intact transcriptional pathway was always observed (Figure 2B). We also tested the transcriptional inducibility of the *RAD9*, *RAD24*, *RAD17* and *MEC3* checkpoint genes themselves. Although *RAD9* was clearly non-inducible, we found that *RAD24*, *RAD17* and *MEC3* were slightly (~2-fold) UV inducible in a manner that was also dependent on an intact checkpoint pathway (data not shown). This, together with the inducibility of *RAD53* and *DUN1* (Figure 2A), suggests a degree of positive feedback regulation within this pathway.

The rad9Δ–rad24Δ double mutant abolishes any residual transcriptional response after UV damage

In all the single mutants tested, the genes of the DDR, in particular *RNR1, RAD52* and *CDC9*, showed residual induction after UV radiation (Figure 2B). This residual induction was not detected in *rad9*Δ–*rad24*Δ cells (Figure 2B). Statistical analysis of the levels of induction of these three transcripts in *rad9*Δ and *rad24*Δ single mutants compared with *rad9*Δ–*rad24*Δ cells demonstrated significant differences. Thus, the *RAD9* and *RAD24* genes also function separately and additively in the transcriptional response to DNA damage.

In wild-type cells, elevated levels of Rad9, Rad24, Rad17 or Mec3 have minor effects on the G_2/M checkpoint after DNA damage and no effect on cell-cycle progression

We used overexpression analysis both to address the possibility that *RAD9* and the *RAD24* epistasis groups are interconnected and also in an attempt to order their function. First, we examined the G_2/M checkpoint after UV irradiation of exponentially growing wild-type cells transformed with vectors in which the *RAD9*, *RAD24*, *RAD17* and *MEC3* checkpoint genes were placed under the transcriptional control of the inducible *GAL1* promoter. In all cases, the presence of high levels of the encoded proteins was confirmed by Western blotting (data not shown). We observed that the normal wild-type G_2/M checkpoint and cell survival responses to UV irradiation were only modestly perturbed by elevated levels of Rad9, Mec3, Rad24 and Rad17 (Figure 3). Furthermore, increased levels of these proteins in wild-type cells did not affect growth or cell-cycle kinetics measurably (data not shown).

Elevated levels of Rad9, or any one of Rad24, Rad17 or Mec3, rescue the G_2/M checkpoint and survival phenotypes observed in null mutants of both the RAD9 and the RAD24 epistasis categories

We next examined the effects of overexpression of *RAD9* or three of the known members of the *RAD24* epistasis group in cells harbouring null mutations in these genes. (i) *RAD9* overexpression not only rescued the G_2/M checkpoint and survival defects observed in *rad9*Δ cells, but also suppressed these defects in *mec3*Δ, *rad24*Δ and *rad17*Δ cells (Figure 3B, and compare with the curves for the respective single mutants in Figure 3A, D, G and J). Interestingly, in *rad24*Δ cells containing overproduced Rad9, the G_2/M checkpoint was ~50% more marked than the wild-type (Figure 3B). (ii) We obtained similar results with *MEC3* overexpression. Both the G_2/M checkpoint (Figure 3E) and survival defects (Figure 3F) observed in *rad9*Δ, *rad17*Δ, *rad24*Δ and *mec3*Δ cells were significantly complemented. [Although *MEC3* overexpression only fully rescued the G_2/M checkpoint in *mec3*Δ cells, in *rad9*Δ, *rad24*Δ and *rad17*Δ cells 66–75% rescue relative to the wild-type was observed (Figure 3E).] In addition, *MEC3* overexpression somewhat delayed exit from the G_2/M checkpoint in *rad24*Δ and *rad17*Δ cells, but not in *rad9*Δ cells (Figure 3E). (iii) *RAD24* overexpression fully rescued the G_2/M checkpoint deficiency associated with its own null mutant and significantly rescued (81%) this defect in *rad9*Δ cells (Figure 3H), thereby indicating that another member of the *RAD24* epistasis group can bypass checkpoint deficiencies associated with null mutation of *RAD9*. *RAD24* overexpression suppressed the survival defects of all mutants to significant extents (Figure 3I). The G_2/M checkpoint rescue in *rad17*Δ (56% rescue) and *mec3*Δ (49% rescue) mutants was less than that obtained with *MEC3* and *RAD9* overexpression (Figure 3B and E). (iv) Overexpression of *RAD17* significantly complemented

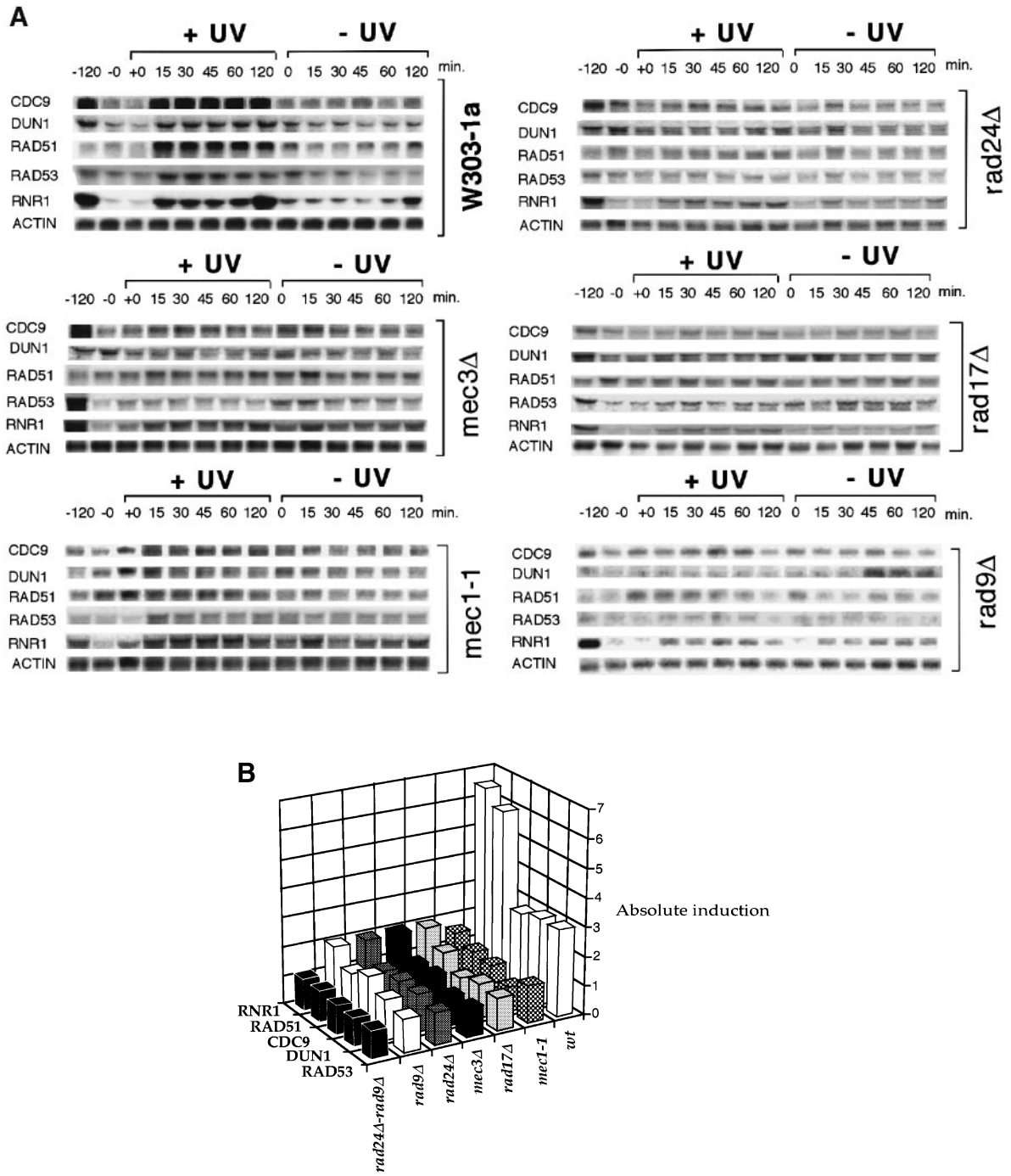

Fig. 2. Transcriptional analysis of DNA damage-inducible genes in wild-type and *rad9*Δ, *rad24*Δ, *rad17*Δ, *mec3*Δ and *mec1-1* cells. (**A**) Exponentially growing cells in YPD medium were arrested in G_1 with α-factor (20 μg/ml) and one half of the culture was UV irradiated (45 J/m^2). Samples were collected at different periods as indicated in the figure, for RNA extraction and Northern blot analyses. Gene probes are as indicated to the left of each Northern blot. Cells were maintained in G_1 throughout the experiment. (**B**) Quantitation of transcriptional induction for each transcript in the different cell types. Each time point was normalized with respect to the value obtained for the *ACT1* loading control. These were then normalized to the value obtained at time 0. The maximum normalized value obtained after irradiation was then divided by the normalized value for the same time point without irradiation, and these values were plotted on a three-dimensional graph. For the *RNR1*, *RAD51* and *CDC9* transcripts, analysis of variance (ANOVA) of data from three independent experiments was performed. Individual means were compared using the LSD range test. In all cases, we observed significant differences in these values between single and double mutants, $P \leqslant 0.05$. Maximum differences were observed with the *RNR1* transcript.

the G_2/M checkpoint and survival defects associated with the *rad17*Δ and *rad9*Δ backgrounds (~90% rescue in both cases). Interestingly, with the *rad24*Δ and *mec3*Δ mutants (Figure 3K and L), no significant rescue of the G_2/M checkpoint defect was observed, suggesting that *RAD17* requires both *RAD24* and *MEC3* for transduction of the damage signal. (v) The *RAD53* gene is believed to function downstream of the *RAD9* and *RAD24* epistasis groups in the DNA damage response pathway (Navas *et al*., 1996; Sanchez *et al*., 1996), although the relative position of *MEC1* has not been determined precisely. Overexpression of *RAD9* or *RAD24* did not rescue the UV sensitivities

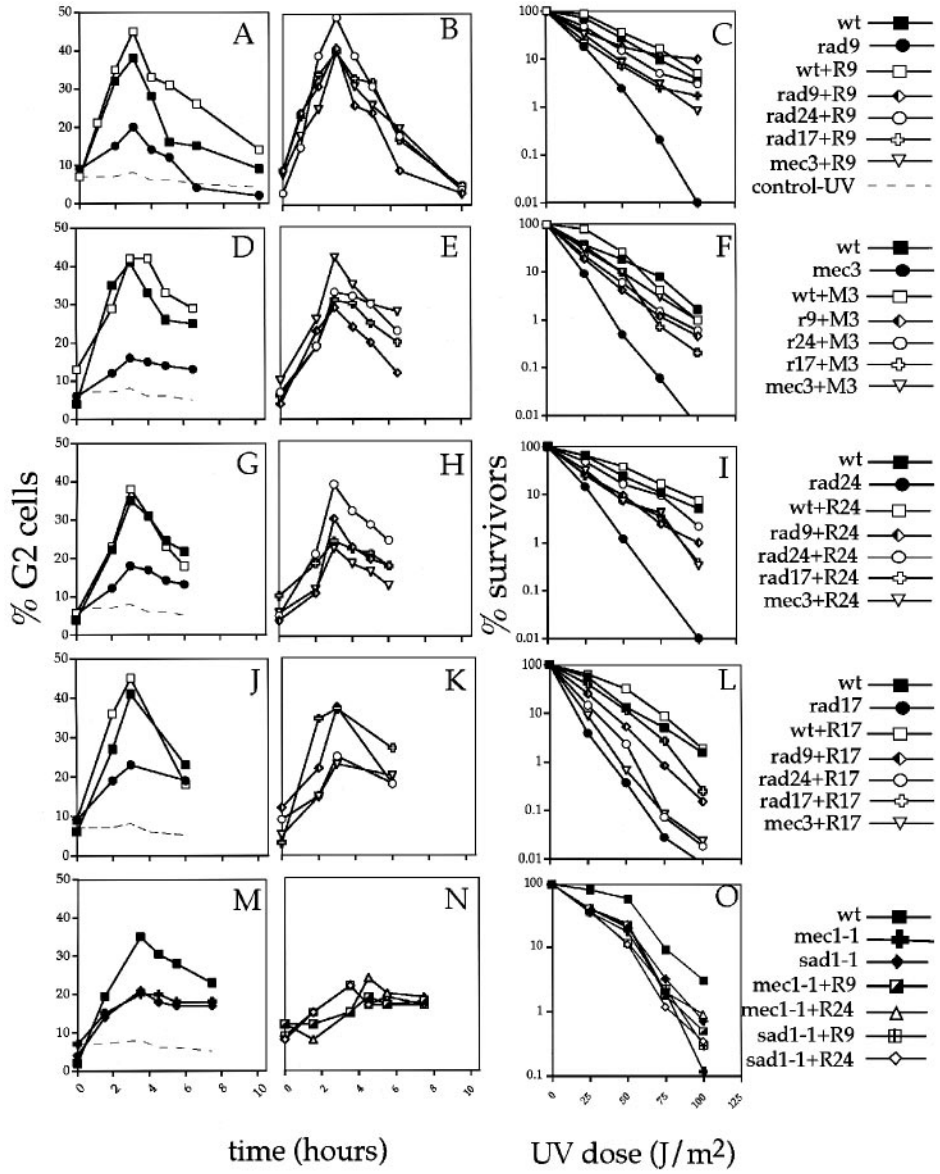

Fig. 3. Rescue of the G_2 checkpoint and UV sensitivity phenotypes by overexpression of *RAD9*, *MEC3*, *RAD24* and *RAD17* in single mutant backgrounds. The percentage of G_2-arrested cells after UV irradiation was determined in wild-type, *rad9*Δ, *rad24*Δ, *rad17*Δ and *mec3*Δ exponentially growing cultures after continuous overproduction of Rad9 (**A** and **B**), Mec3 (**D** and **E**), Rad24 (**G** and **H**) and Rad17 (**J** and **K**) in each mutant background. The first panel of each pair shows for comparison the proportion of G_2 cells after UV irradiation of wild-type and single mutant cells. Note that in each case the curves for the *rad9*Δ, *mec3*Δ, *rad24*Δ and *rad17*Δ single mutants are highly similar. Also shown for comparison is a control unirradiated culture (dashed line). The residual G_2/M checkpoint in *mec1-1* and *sad1-1* cells is shown in (**M**), and the effects of overproduction of Rad9 and Rad24 in *sad1-1* and *mec1-1* cells are shown in (**N**). The percentage of survivors after different UV doses scored in wild-type, *rad9*Δ, *rad24*Δ, *rad17*Δ and *mec3*Δ cells after overproduction of Rad9, Mec3, Rad24 and Rad17 is indicated in (**C**), (**F**), (**I**) and (**L**) respectively. UV survival after overproduction of Rad9 and Rad24 in *sad1-1* and *mec1-1* mutants is shown in (**O**). Continuous overexpression of checkpoint proteins was achieved by growing cells in YNB plus 2% raffinose and 2% galactose. Every experiment was repeated at least three times, and platings were carried out on the same day in triplicate. Note that the scale of the *y* axis in (O) is changed for clarity, as both the *mec1-1* and *sad1-1* mutants have less pronounced UV sensitivities than we observed in the null checkpoint mutants tested.

(Figure 3O) or G_2/M checkpoint defects (compare Figure 3M and N) observed in *sad1-1* (an allele of *RAD53*) and *mec1-1* cells, suggesting that *MEC1* functions downstream of *RAD9* and the *RAD24* epistasis group. Neither of these mutations completely abrogate the G_2/M checkpoint (Figure 3M), most likely because they may be hypomorphic alleles retaining partial function. However, a *MEC1*- and *RAD53*-independent contribution to this checkpoint is formally possible.

In summary, all known members of the *RAD24* epistasis group can bypass defects caused by the *rad9*Δ mutation and, reciprocally, *RAD9* overexpression can bypass null mutations in the *RAD24* epistasis group efficiently. However, the checkpoint defects and UV sensitivity of *sad1-1* and *mec1-1* cells cannot be overridden by overexpression of either *RAD9* or *RAD24*, demonstrating that *RAD53* and *MEC1* are essential components downstream of *RAD9* and the *RAD24* epistasis group of genes for these phenotypes.

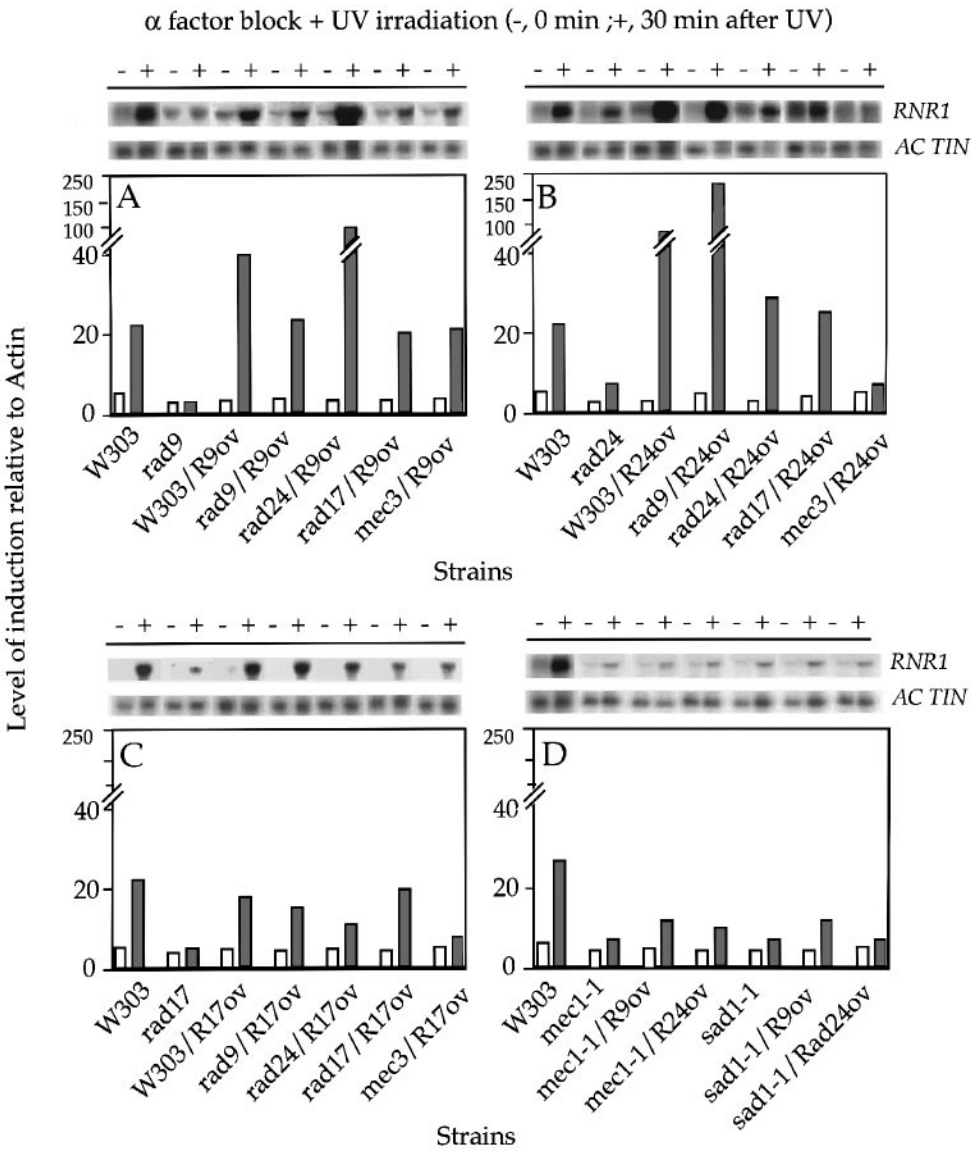

Fig. 4. Transcription induction of the *RNR1* gene after overexpression of *RAD9*, *RAD24* or *RAD17* in wild-type, *rad9*Δ, *rad24*Δ, *rad17*Δ and *mec3*Δ cells. (**A**) *RAD9* overexpression; (**B**) *RAD24* overexpression; (**C**) *RAD17* overexpression; (**D**) overexpression of *RAD9* and *RAD24* in the *mec1-1* and *sad1-1* mutants. In (A–D) we also show for comparison the transcriptional inductions obtained with the wild-type and the appropriate single mutant. Experimental procedures were as for Figure 1. Cells arrested in G_1 prior to UV irradiation are indicated by a minus symbol above each panel and by open rectangles within each panel. G_1-arrested cells harvested 30 min after UV irradiation with maintenance of the G_1 block are indicated by the plus symbol above each panel and by the closed rectangles within each panel. The levels of induction are relative to the *ACT1* loading control. Note that the eighth and tenth lanes in (B) are underloaded. As before, overproduction of either Rad9 or Rad24 was confirmed by Western blotting.

Overproduced Rad9 or Rad24 rescues the defect in the transcriptional response to DNA damage observed in null mutants of both RAD9 and the RAD24 epistasis category

We analysed the induction of the DDR in G_1-arrested checkpoint mutants in which *RAD9* and *RAD24* were overexpressed continuously from the *GAL1* promoter. Transcripts were examined prior to, and 30 min after, UV irradiation. Figure 4 shows the results obtained with the *RNR1* transcript, but qualitatively similar results were also obtained for *CDC9* and *RAD53* (data not shown). *RAD9* and *RAD24* overexpression not only rescued the defect in the transcriptional response observed in their own null mutant backgrounds, but slightly enhanced (2- to 3-fold) the response observed in wild-type cells (Figure 4A and B), suggesting that they are somewhat rate limiting for this response. *RAD9* overexpression resulted in rescue of the transcriptional induction defect found in null mutations of all tested members of the *RAD24* epistasis group to wild-type levels (Figure 4A). Although *RAD24* overexpression complemented the transcriptional induction defect observed in the *rad24*Δ and *rad17*Δ strains to the same level as found in the wild-type (Figure 4B), it did not rescue the defect seen in *mec3*Δ cells. *RAD17* overexpression complemented the transcriptional defect in its own null mutant to near wild-type levels and the defect in *rad9*Δ cells to ~70% of wild-type levels (Figure 4C). However, it only weakly rescued the transcriptional defect of *rad24*Δ cells (50% rescue) and did not significantly rescue this defect in *mec3*Δ cells (Figure 4C). Unlike *RAD9* and *RAD24* overexpression, *RAD17* overexpression did not cause an increase in transcription in the wild-type

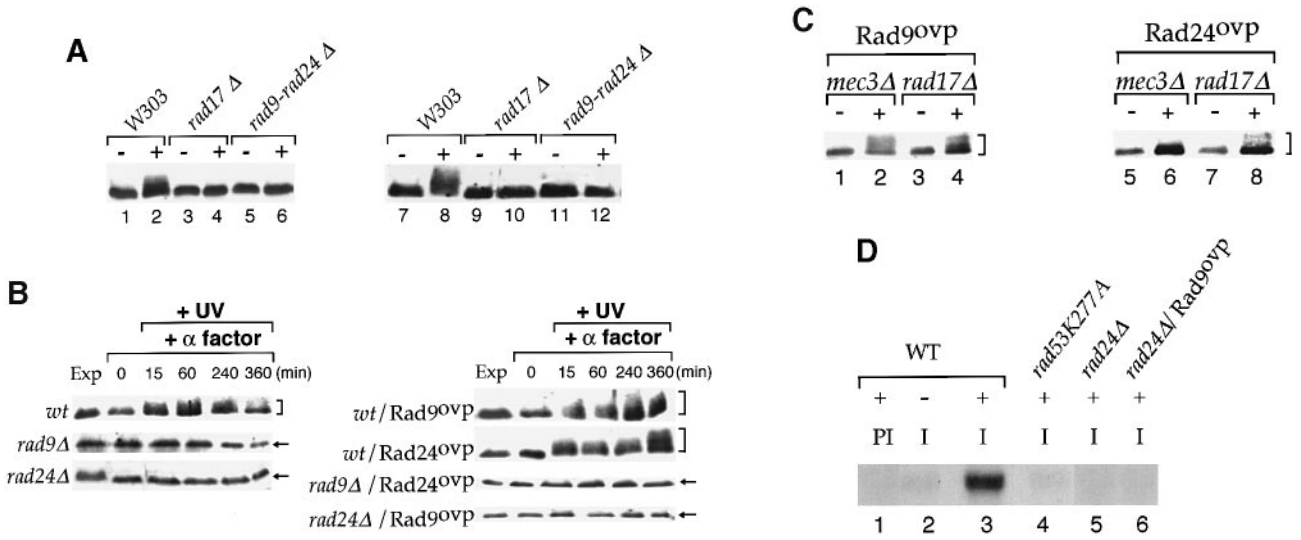

Fig. 5. Analysis of Rad53 phosphorylation and kinase activity in checkpoint mutant cells with or without overexpression of *RAD9* or *RAD24*. (**A**) Cells arrested in G_1 with α-factor (lanes 1–6) were UV treated (+) or mock treated (–) and analysed for Rad53 phosphorylation 30 min after irradiation. Cells arrested in G_2 with nocodazole (lanes 7–12) were UV irradiated (+) or mock treated (–) and analysed for Rad53 phosphorylation 30 min after irradiation. (**B**) G_1-arrested cells as indicated were UV irradiated either in the presence or absence of overproduced Rad9 or Rad24 and samples analysed at the times shown. Exp indicates exponentially growing cells. (**C**) G_1-arrested *mec3*Δ and *rad17*Δ cells with overproduced Rad9 and Rad24 as indicated were UV irradiated (+) or mock treated (–) and analysed for Rad53 phosphorylation 60 min after the time of irradiation. Arrows indicate hypophosphorylated Rad53 and brackets the modified forms. (**D**) Cells as indicated were arrested in G_1 with α factor, UV treated (+) or mock treated (–) and extracts precipitated with either anti-Rad53 immune (I) or pre-immune (PI) sera. The washed pellets were then used in histone H1 kinase assays as described.

background, suggesting that it is not rate limiting for the transcriptional response. A very striking result was obtained when *RAD9* was overexpressed in *rad24*Δ cells, or when *RAD24* was overexpressed in *rad9*Δ cells (Figure 4A and B). Elevated Rad9 levels in *rad24*Δ cells caused a 35-fold transcriptional induction relative to unirradiated cells of *RNR1* after UV irradiation (Figure 4A). Similarly, elevated Rad24 levels in *rad9*Δ cells caused this induction to be increased to 46-fold (Figure 4B). Wild-type cells typically show a 6-fold induction of *RNR1* after UV irradiation of G_1-arrested cells (Figure 4A–D). These data can be explained by negative regulatory interactions between *RAD9* and *RAD24*. As the enhanced transcriptional response observed when *RAD9* is overexpressed in *rad24*Δ cells is not apparent in *rad17*Δ and *mec3*Δ cells (Figure 4A), nor is it observed after *RAD17* overexpression in any of the mutant backgrounds (Figure 4C), these interactions appear to be specific to *RAD24* and *RAD9*. Finally, overexpression of *RAD9* or *RAD24* did not bypass the transcriptional induction defect seen in *mec1-1* and *sad1-1* mutant cells (Figure 4D), once more placing *MEC1* and *RAD53* function downstream of the *RAD9* and *RAD24* epistasis categories.

Modification and activation of the Rad53 protein after damage is dependent on RAD9, RAD24, RAD17 and MEC3 and requires the simultaneous presence of both Rad9 and Rad24

Rad53 is phosphorylated in a *RAD9*-dependent manner under conditions in which G_1 synchronized cells are UV irradiated and immediately released from the G_1 block (Navas *et al*., 1996). Similar modification of Rad53 has also been shown to be *MEC3* dependent after methylmethane sulfonate (MMS) treatment of cells blocked in G_2 with a microtubule inhibitor (Sun *et al*., 1996). This DNA damage-dependent modification of Rad53 is *MEC1* dependent (Sanchez *et al*., 1996), but its significance is not well understood. Treatment of cells with hydroxyurea, an inhibitor of DNA synthesis, results in Rad53 phosphorylation accompanied by a modest increase in its kinase activity (Sun *et al*., 1996), and Rad53 kinase activity has been shown to be required for full checkpoint pathway function (Fay *et al*., 1997; Kim and Weinert, 1997).

We examined Rad53 modification after UV irradiation in wild-type and checkpoint mutant cells continuously blocked in G_1 or in G_2. As phosphorylation of Rad53 is known to be cell-cycle regulated close to the G_1/S boundary (Sun *et al*., 1996), these experiments focus on damage-dependent modification of Rad53 independent of cell-cycle position. Essentially identical results were obtained for the G_1 and G_2 block experiments (Figure 5A). In both experiments, the DNA damage-dependent modification of Rad53 is clearly evident in wild-type cells 30 min after UV irradiation as more slowly migrating bands (lanes 2 and 8). However, in *rad17*Δ (lanes 4 and 10) and *rad9*Δ–*rad24*Δ double mutant cells (lanes 6 and 12), this modification was not detectable. In addition, Rad53 modification was not detected in *rad9*Δ, *rad24*Δ (Figure 5B) or *mec3*Δ cells (data not shown). To determine whether modification of Rad53 correlates with activation of Rad53 as a kinase, we performed histone H1 kinase assays with Rad53 immunoprecipitates (Figure 5D). Rad53 kinase activity was detected after UV irradiation in wild-type cells (lanes 3), but not in *rad24*Δ (lane 5) or in *rad9*Δ (data not shown) cells, and correlated with phosphorylation of Rad53 (compare Figure 5A and B with D). This kinase activity is Rad53- and UV-specific because it is not detectable in irradiated pre-immune precipitates (lane 1) nor in unirradiated immunoprecipitates (lane 2). Further-

more, it is not detectable in an irradiated immunoprecipitate from a strain carrying an apparently 'kinase-dead' allele of *RAD53*, *rad53K277A* (lane 4). Similar results were obtained by examining Rad53 autophosphorylation (data not shown). Thus, detectable damage-dependent modification of Rad53 in G_1- or G_2-blocked cells is dependent on intact *RAD9* and *RAD24* branches of the DNA damage checkpoint pathway, and this modification results in activation of Rad53 kinase.

In Figure 4, we present results that suggest specific antagonistic interactions between *RAD9* and *RAD24*. The phosphorylation of Rad53 is another cellular response to DNA damage downstream of *RAD9* and the *RAD24* epistasis group. We examined this modification in UV-irradiated cells that were held in G_1 in the presence of overproduced Rad9 or Rad24. Overproduction had no effect on Rad53 modification in the absence of DNA damage (data not shown). In wild-type cells, the modification of Rad53 first appears immediately after irradiation, seems to peak at 60 min, but is still detectable after 6 h (Figure 5B). When either Rad9 or Rad24 were overproduced in wild-type cells, the phosphorylated form of Rad53 also appeared immediately after irradiation but then continued to accumulate to high levels for the duration of the experiment (Figure 5B). In *rad9*Δ or *rad24*Δ cells, no Rad53 modification is detectable (Figure 5B), and this phenotype can be rescued by overproduction of Rad9 or Rad24 respectively (data not shown). Rad9 overproduction can bypass the defect in Rad53 modification after damage found in *mec3*Δ and *rad17*Δ (Figure 5C, lanes 1–4). Similarly, Rad24 overproduction rescues this defect in *rad17*Δ (Figure 5C, lanes 7 and 8). However, Rad9 overproduction in *rad24*Δ cells or Rad24 overproduction in *rad9*Δ cells did not rescue the defect in Rad53 modification after UV irradiation (Figure 5B), although the G_1/S checkpoint (data not shown), the transcriptional response (Figure 4), the G_2/M checkpoint (Figure 3) and cellular viability (Figure 3) were restored under these conditions. These data suggest that under these conditions Rad9 and Rad24 are required simultaneously for Rad53 phosphorylation. The lack of Rad53 phosphorylation in *rad24*Δ cells overexpressing *RAD9* correlates with a lack of kinase activity in these cells (Figure 5D, lane 6), indicating that Rad53 kinase activity is not required for functioning of the checkpoint pathway under these conditions. Interestingly, Rad24 overproduction did not rescue Rad53 modification in *mec3*Δ cells (Figure 5C). This final observation is consistent with our previous data demonstrating that Rad24 overproduction cannot restore the G_2 checkpoint (Figure 3) or the transcriptional response (Figure 4) in *mec3*Δ cells, and supports the hypothesis that *MEC3* functions downstream of *RAD24* within this epistasis group.

Discussion

RAD9 and RAD24 define two converging branches of the DNA damage checkpoint that function additively to produce most of the checkpoint signal

RAD9, *RAD24*, *RAD17*, *MEC3* and *DDC1* are thought to be involved in a signalling cascade that links damaged DNA to presumptive signal transducing kinases encoded by *MEC1* and *RAD53*. These kinases then regulate, via poorly understood mechanisms, the downstream biological effects of the DNA damage-dependent checkpoint pathway, namely cell-cycle delay, transcription of the DDR and possibly DNA repair (for a recent review, see Elledge, 1996). *RAD24*, *RAD17*, *MEC3* and *DDC1* have been placed into an epistasis group distinct from *RAD9* with respect to their UV or X-ray sensitivity phenotypes (Eckardt Schupp *et al*., 1987; Lydall and Weinert, 1995; Longhese *et al*., 1997). Epistasis categories are usually indicative of distinct biochemical pathways; however, both *RAD9* and the *RAD24* epistasis group are required for efficient cell-cycle arrest after DNA damage in G_1/S (Siede *et al*., 1993) and G_2/M (Weinert and Hartwell, 1988; Weinert *et al*., 1994; Yang *et al*., 1997; see also Figures 1 and 3). Both epistasis groups are also required after damage for efficient induction of the DDR (Figure 2), which includes *RAD53* and phosphorylation of the Rad53 protein (Figures 2 and 5A). These data are best interpreted by the assumption that *RAD9* and the *RAD24* epistasis group define biochemically distinct branches of the DNA damage-dependent checkpoint pathway. These branches probably function at, or close to, DNA damage and subsequently converge. The point of convergence is thought to be at or above *MEC1*, with *RAD53* functioning downstream, as Rad53 overproduction suppresses the *mec1-1* allele and Rad53 phosphorylation after damage depends on *MEC1* function (Sanchez *et al*., 1996). Our data place *RAD9* and the *RAD24* epistasis group upstream of *MEC1*, as overexpression of either *RAD9* or *RAD24* cannot rescue the G_2/M checkpoint (Figure 3M and N), the UV sensitivity (Figure 3O) or the defect in the transcriptional response to DNA damage (Figure 4C) observed in *mec1-1* strains. Additionally, the transcriptional induction after UV treatment of *RAD53* itself is severely affected in a *mec1-1* mutant (Figure 2).

That each upstream branch of the DNA damage-dependent checkpoint pathway is partially redundant and quantitatively equivalent in terms of the signal transduced from damaged DNA is demonstrated by two observations. First, *RAD9* overexpression can bypass mutations in the *RAD24* epistasis group and members of the *RAD24* epistasis group are capable of bypassing deficiencies in *RAD9* for checkpoint, survival and transcription phenotypes (Figures 3 and 4). Secondly, single mutants in either branch have indistinguishable phenotypes with respect to the transcriptional induction of the DDR (Figure 2), checkpoints (both G_1/S and G_2/M, Figures 1 and 3) and survival after damage (Figure 3). It is particularly interesting that after UV damage a *rad9*Δ–*rad24*Δ double mutant has no detectable transcriptional induction of the DDR (Figure 2B), has no apparent G_1/S checkpoint (Figure 1), only a residual G_2/M checkpoint (Figure 2), and is more sensitive to DNA damage than either single mutant (Eckardt Schupp *et al*., 1987; Lydall and Weinert, 1995; our unpublished observations). Similarly, the *rad9*Δ–*mec3*Δ double mutant is also more defective in the G_1/S and G_2/M checkpoints and has an additively worse *rad* phenotype than either single mutant (data not shown). These data suggest that the two branches are responsible for the majority of the signal emanating from damaged DNA. The remaining G_2/M checkpoint observed in these double mutants is probably due to S-phase-specific pathways (Navas *et al*., 1996).

Using overexpression analysis, we observed a hierarchy of suppression phenotypes within the *RAD24* epistasis group (Figure 3). Overexpression of *MEC3* is the most effective at rescuing the G_2/M checkpoint, followed by *RAD24* and then *RAD17*. Thus it is likely that Rad17 requires both Rad24 and Mec3 for function, suggesting that the *RAD24* epistasis group of genes can be functionally ordered with *RAD17* and *RAD24* upstream of *MEC3*. This ordering within the *RAD24* epistasis group is supported by the following observations. Overexpression of *RAD17* is not very effective at rescuing the survival defect of *rad24*Δ and, particularly, *mec3*Δ cells. Similarly, it cannot rescue the deficiency in the transcriptional response to DNA damage of *mec3*Δ cells and appears to rescue this defect weakly in *rad24*Δ cells (Figure 4C). *RAD24* overexpression cannot rescue the DNA damage-dependent phosphorylation of Rad53 in *mec3*Δ cells and only weakly rescues this modification in *rad17*Δ cells (Figure 5C). Such functional ordering does not necessarily preclude a previously proposed model which puts the gene products of the *RAD24* epistasis group into a putative protein complex (Lydall and Weinert, 1995), nor does it imply that there is a strictly linear relationship between the members of the *RAD24* epistasis group. Indeed, we have observed slightly less penetrant checkpoint and survival phenotypes with *rad9*Δ–*mec3*Δ cells compared with *rad9*Δ–*rad24*Δ cells, consistent with a degree of non-linearity of function within this group of genes. On the other hand, the more penetrant phenotypes observed with the *rad9*Δ–*rad24*Δ mutant, compared with the *rad9*Δ–*mec3*Δ mutant, may be due, at least in part, to loss of specific *RAD9–RAD24* interactions (see below). The data discussed above support the model outlined in Figure 6. *RAD9* and the *RAD24* epistasis group are placed onto two separate branches of the signalling pathway, upstream of *MEC1* and *RAD53*, with both normally contributing equally to the signal sent from damaged DNA. Resolution of the details of this pathway will require future biochemical investigation.

We have shown that cells harbouring a single null mutation in any of *RAD9*, *RAD17*, *RAD24* and *MEC3*, or the previously isolated alleles of *RAD53* and *MEC1*, *sad1-1* and *mec1-1* respectively, have a severely diminished transcriptional response to DNA damage. Previously, using cells partially deficient in nucleotide excision repair, Kiser and Weinert (1996) described *RAD53*- and *MEC1*-dependent transcriptional induction of *RNR3* after UV irradiation, but they observed only partial dependency upon *RAD9* and the *RAD24* epistasis group. However, an independent study indicated that *RNR3* induction after DNA damage was highly dependent on *RAD9*, *RAD24* and *MEC3* (Navas *et al*., 1996). Furthermore, essentially identical residual G_1/S and G_2/M checkpoints are observed in all the single mutants we have tested (Figures 1 and 3, and data not shown). Our data indicate that any of the disruptions to the DNA damage-dependent checkpoint pathway we have used result in a quantitatively similar defect in the transcriptional as well as the checkpoint responses to DNA damage. Interestingly, all the checkpoint genes tested in this study appear to control the damage-dependent transcriptional induction of *RAD53* itself, and also of *DUN1* (Figure 2). Both encode related protein kinases with roles in the cellular response to DNA damage (Zhou and Elledge, 1993; Allen *et al*., 1994; Sun *et al*., 1996); *RAD53* has roles in all known responses whereas *DUN1* is thought to function primarily in regulating the transcriptional response to damage of the *RNR1*, *2* and *3* genes. [However, recent evidence suggests that *DUN1* also has a significant role in checkpoint regulation (Pati *et al*., 1997).] Thus a degree of positive feedback regulation of the checkpoint pathway is possible. This possibility is further supported by the reproducible, albeit only 2-fold, transcriptional induction after UV irradiation of *RAD24*, *RAD17* and *MEC3* (data not shown).

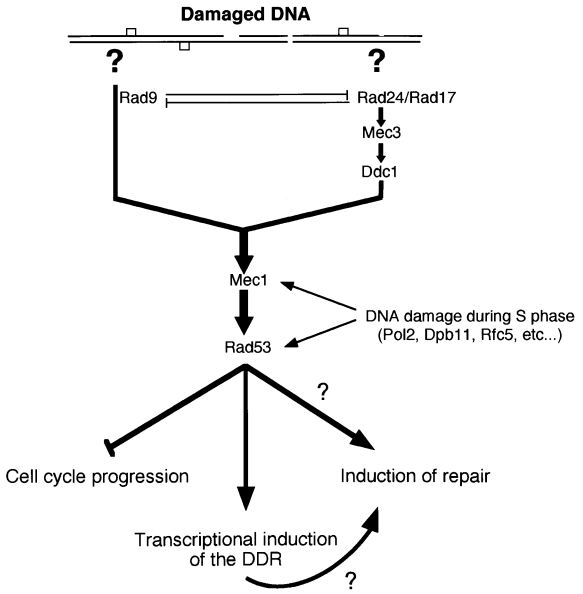

Fig. 6. Organization of the major DNA damage-dependent checkpoint pathway of *S.cerevisiae*. Shown below the schematic of damaged DNA are the pathways defined by Rad9 and Rad24. The biochemical details of how either of these pathways sense and/or signal DNA damage are not known. Currently, no other members of the Rad9 branch of this pathway have been identified, but the Rad24 branch can be ordered as shown, although strict linearity of function within this branch is unlikely. Ddc1, a recently identified member of the Rad24 branch, can be placed downstream of Mec3 as overexpression of Ddc1 partially rescues *mec3*Δ function but Mec3 overexpression cannot rescue *ddc1*Δ (Longhese *et al.*, 1997). Also shown are the antagonistic interactions specific to Rad9 and Rad24. Both the Rad9 and Rad24 branches converge on the Mec1 and Rad53 protein kinases which may function in signal transduction as a kinase cascade. (Note that Tel1 and Dun1, which are not shown, may be partially redundant functional homologues of Mec1 and Rad53 respectively.) The biological consequences downstream of Rad53 due to activation of this pathway are indicated. It is unclear at present whether induction of efficient repair requires the transcriptional induction of the DDR or whether there is a contribution from checkpoint pathway-dependent post-transcriptional mechanisms. During S phase, the Rad9 and Rad24 pathways are believed to be only minor contributors to sensing DNA damage, whereas the other possible pathways indicated appear to have a more important role.

Evidence for specific genetic interactions between RAD9 and RAD24 required for phosphorylation and activation of Rad53

We made an unexpected observation while studying the effects of overexpression of *RAD9* or *RAD24* on the transcriptional response to DNA damage. A dramatically increased transcriptional response was observed when *RAD9* was overexpressed in *rad24*Δ cells (Figure 4A). This result indicates that *RAD9* can act negatively on

RAD24. Lydall and Weinert (1995) have also obtained evidence that *RAD9* acts negatively on *RAD24*. Any effects of *RAD9* on *RAD17* or *MEC3* were not examined in their study. Their observation has led to the model that Rad9 functions as a negative regulator of a *RAD24*-dependent exonuclease activity, although its role is unlikely to be limited to negative regulation as null mutants of *RAD9* and *RAD24* have similar phenotypes and *RAD9* overexpression rescues *rad24*Δ phenotypes (Figure 3). Using the transcriptional response to DNA damage, it was also possible for us to obtain the reciprocal result, i.e. *RAD24* acts negatively on *RAD9* function. Removal of *RAD9* from cells in which *RAD24* was overexpressed caused a similarly dramatic increase in the transcriptional response in comparison with the response in wild-type cells (Figure 4B). Interestingly, the antagonistic effect observed between *RAD9* and *RAD24* was specific for these two genes. Overexpression of *RAD9* in *rad17*Δ and *mec3*Δ cells, or overexpression of *RAD17* in *rad9*Δ cells, did not cause an enhanced transcriptional response (Figure 4A and C). The antagonism between *RAD9* and *RAD24* that we have observed by examination of the transcriptional response to DNA damage seems surprising as we do not see dramatic rescue of other phenotypes under these conditions (Figure 3). A possible explanation for these observations may be that the dramatic transcriptional rescue phenotypes are related to conditions in which the cell cycle is arrested. This hypothesis is supported by our observation that antagonism between *RAD9* and *RAD24* in the transcriptional response is difficult to detect in asynchronous, exponentially growing cells (M.-A.de la Torre-Ruiz, unpublished results). Significantly, the *cdc13* single-stranded DNA accumulation assay used by Lydall and Weinert (1995) also involves cell-cycle arrest, this time in G_2. Thus, in the absence of cell cycling, the antagonistic interactions specific to *RAD9* and *RAD24* may be detected more easily. Nevertheless, evidence that such antagonism can occur in cycling cells comes from the observation of an enhanced (50% greater) G_2 checkpoint when *RAD9* was overexpressed in *rad24*Δ cells (Figure 3B).

Support for the specific genetic interaction between *RAD9* and *RAD24* also comes from our studies of Rad53 modification after DNA damage. UV irradiation of wild-type cells causes modification of Rad53 (Figure 5A), activation of its kinase activity (Figure 5D), checkpoint arrest in both G_1/S and G/M (Figures 1 and 3) and transcriptional induction of the DDR (Figure 2). The UV-dependent modification of Rad53 is not detectable in any single mutants arrested in G_1. Furthermore, *rad24*Δ cells do not have detectable Rad53 kinase activity under these conditions (Figure 5D); nevertheless, single checkpoint mutants have residual G_1 checkpoint activity and there is residual induction of the DDR. These residual activities are due either to undetectable but sufficient phosphorylation and activation of Rad53 kinase or to unknown *RAD53*-independent mechanisms. In the *rad9*Δ–*rad24*Δ double mutant, modification of Rad53 and its kinase activity are also undetectable, but residual checkpoint and transcriptional induction are now abolished. This may be explained by complete loss of Rad53 activation or by the absence of *RAD53*-independent mechanisms in the double deletion. Support for the latter of these possibilities comes from the observation that Rad53 kinase activity in single and double mutants is as low as in an apparently 'kinase-dead' allele of *RAD53*, *rad53K227A* (Figure 5D).

The lack of detectable Rad53 phosphorylation after UV irradiation of the single mutants can be rescued in most cases by overexpression of *RAD9* or *RAD24*. The principal exception to this occurred when Rad9 was overproduced in *rad24*Δ cells or Rad24 in *rad9*Δ cells. Under these conditions, neither Rad53 modification nor its kinase activity are detectable (Figure 5). This is despite full, or even greater than full, activity of the checkpoint pathway under these conditions, as measured by survival (Figure 3), the G_1/S checkpoint (data not shown), the G_2/M checkpoint (Figure 3) and the transcriptional response (Figure 4). Thus the downstream consequences of checkpoint pathway activation are not always dependent on wild-type levels of activation of *RAD53* function, suggesting that under certain conditions this function can be bypassed. This bypass may allow partial rescue of checkpoint function when one of the two upstream branches of the checkpoint pathway is perturbed (the single mutants). A more pronounced bypass is observed, again without Rad53 phosphorylation and activation, in the absence of antagonistic interactions between *RAD9* and *RAD24* together with overproduction of either Rad9 or Rad24. Interestingly, the regulation of a downstream effector of the G_2 checkpoint, *PDS1*, has recently been shown to be *RAD53* independent (Cohen-Fix and Koshland, 1997). Furthermore, *DUN1* is a partial functional homologue of *RAD53* for checkpoint function and there is some evidence for an alternative checkpoint pathway in budding yeast that can be activated by expression of a human cDNA, CHES1 (Pati *et al*., 1997). Thus *DUN1*-dependent mechanisms or even alternative pathways could conceivably be used for *RAD53* bypass under some circumstances. However, the biochemical mechanism and biological relevance of the proposed bypass pathway(s) will require future investigation.

In summary, our data indicate that *RAD9* and the *RAD24* epistasis group can be placed onto two branches that converge on the same target. Both branches act in an additive manner, being responsible for most of the checkpoint signal in exponentially growing cells; moreover, they display partial functional redundancy. Additionally, there is evidence for specific antagonistic interaction between *RAD9* and *RAD24* after DNA damage. At least under certain conditions, interaction between *RAD9* and *RAD24* is also required for phosphorylation of Rad53 and activation of Rad53 kinase. Intriguingly, the downstream biological consequences of this pathway are not always correlated with this kinase activity.

Materials and methods

Strain construction

RAD9, *RAD24*, *RAD17* and *MEC3* deletions were generated in the W303-1a background (*Mat**a**; ho; ade2-1; can1-100; his3-11; leu2-3,115; trp1-12; ura3*), using the direct gene replacement technique previously described (Baudin *et al*., 1993). The *URA3* marker was used to delete *RAD24*, *RAD17* and *MEC3*, whereas *RAD9* was deleted with *HIS3*. We used the following specific oligos corresponding to the 5′- and 3′-terminal coding sequences of the genes to be deleted (upper case) followed by 17–21mers designed to anneal the selected marker (either *URA3* or *HIS3*) to be deleted (lower case). RAD9: sense oligo, 5′-

TCTTCAACATCAGGGCTATGTCAGGCCAGTTAGTTCAATGGAA AAGCTCTCatgcggcatcagagcag-3′; antisense oligo, 5′-TAATTTCAT-CTAACCTCAGAAATAGTGTTGTATATATCATTGTCCGTAATcttacg-catctgtgcgg-3′. RAD24: sense oligo, 5′-ATGTACAAGAAGCTTT-AGATGCCATGTTTTTACCTAACGCCAAGCATAGGatgcggcatcagag cag-3′; antisense oligo, AGTTAGAGTATTTCCAGATCTGAATCT-GAAAGG GACTCACTGATAACTGcttacgcatctgtgcgg. RAD17: sense oligo, 5′-GGTGTGGAAACAAAGTAGTTGAAGGATTTCAACTATG-CGAATCAACAATGgattcggtaatctccgaac-3′; antisense oligo, TCTGC-GTTTTCTGCGATGCTGGATATTGACTTAAAAAAATATAGGAATA-Tattgaagctctaatttgtgag. MEC3: sense oligo: 5′-ATGAAATTAAAA-TTGATAGTAAATGGTTGTGAAGCACCTGATGATTATAAgattcggtaa-tctccgaac-3′; antisense oligo, 3′-TACAAGCCCTTCGCTCTTGCTATA-ATATATGATTTGTCCTCTTTCCCattgaagctctaatttgtgag.

PCR fragments were transformed into the strain W303-1a. Transformants selected for URA^+ or HIS^+ prototrophy were checked by UV sensitivity, Southern blotting and diagnostic PCR. Cells were grown in YEPD or minimal medium and plasmids introduced as previously described (Aboussekhra *et al*., 1996). Synthetic α-factor was used at a final concentration of 20 μg/ml in the W303 background. The *sad1-1* and *mec1-1* strains were kind gifts from Ted Weinert (Tucson, AZ) and Errol Friedberg (Dallas, TX). *mec1-1* was backcrossed a further three times into our W303 background, scoring for MMS sensitivity each time. The strain obtained reverts at high frequency and was scored for MMS sensitivity prior to each use. The *sad1-1* strain is in a W303-related background but in all experiments it was also compared with the isogenic parental background, in addition to our W303-1a. Additionally, a *rad53-1* strain behaved identically to *sad1-1* in the transcriptional response.

Plasmids

For cloning the *RAD9*, *RAD24*, *MEC3* and *RAD17* coding sequences under the *GAL1* promoter, we PCR amplified the four open reading frames corresponding to each gene using *Pfu* thermostable DNA polymerase (Stratagene). The amplified fragments were then subcloned into either the *Bam*HI (*RAD9*, *RAD17* and *MEC3*) or the *Spe*I (*RAD24*) sites of YCpIF vectors (Foreman and Davis, 1994) as follows: pGAL-RAD9 (in YCpIF16), sense oligo 5′-CGCGGATCCATGTCAGGCCAGTTA-GTTC-3′ and antisense 5′-CGCGGATCCTCTAACCTCAGAAATAGT-GTTG-3′; pGAL-RAD24 (in YCpIF15), sense oligo 5′-CGTCAAC-TAGTTGATAGTACGAATTTGAACAAACGGCCC-3′ and antisense 5′-CCAGTACTAGTAGTATTTCCAGATCTGAATCTGAAAGGGAC-3′; pGAL-MEC3 (in YCpIF10), sense oligo 5′-CGTCAGGATCCG-AAATTAAAATTGATAGTAAATGG-3′ and antisense 5′-CCAGTGG-ATCCTTACAAGCCCTTCGATCTTGC; pGAL-RAD17 (in YCpIF15), sense oligo 5′-CGTCAGGATCCGCGAATAAACAGTGAGCTAGCG-3′ and antisense 5′-CCAGTGGATCCGTAAAAAATATAGGAATAT-CCTTTGTTGG-3′.

Overexpression of any of these checkpoint genes fully complemented the cell cycle and survival deficiencies after UV irradiation of their own mutant backgrounds, indicative of correct function. Sequence analyses did not reveal any introduced mutations. Overproduction of each encoded protein was confirmed by Western blotting with the 12CA5 monoclonal antibody directed against the haemagglutinin (HA) epitope included in the YCpIF plasmids.

Irradiation procedures, α-factor and nocodazole blocks and survival curves

G_1 blocks with α-factor and UV irradiation were performed as previously described (Aboussekhra *et al*., 1996). For survival curves, cells were grown to log phase (1×10^7 cells/ml), diluted appropriately, plated either in YPD or minimal medium, allowed to dry briefly and then irradiated at the doses indicated. Cells arrested in G_2 after UV were monitored by nuclear and cell morphology. Nuclei were visualized by staining with 4′,6-diamino-2-phenylindole (DAPI, Sigma). Large budded cells corresponding to mother and daughter cells of essentially equivalent volume with the nucleus at the neck of the bud were scored as cells blocked in G_2/M, prior to anaphase. This phenotype is indicative of the G_2/M checkpoint. Fluorescence-activated cell sorting (FACS) analysis was also used to confirm this G_2/M block. An advantage of this method is that the only perturbation to the cultures required is the UV treatment, thereby allowing a more physiological examination of any resulting cell cycle arrest. Nocodazole (Sigma) was prepared in dimethylsulfoxide (DMSO) and used at a final concentration of 5 μg/ml.

Northern blot analysis

Total RNA preparations were performed either by the hot phenol extraction or using the RNeasy Mini Kit (Qiagen). Northern blots were prepared, hybridized and quantitated by phosphorimaging (Molecular Dynamics) all as previously described (Aboussekhra *et al*., 1996).

Rad53 antibody, Western blotting and kinase assay

A C-terminal fragment of Rad53 (amino acids 468–835) was expressed in *E.coli* using the pET21b expression vector. This was affinity purified using a nickel-NTA–agarose column (Qiagen #30410) and used to immunize rabbits. For Western analysis, total yeast protein extracts were run on SDS–PAGE gels with 6.5% acrylamide and 80:1 acrylamide:bis-acrylamide. The rabbit polyclonal serum was used at a final dilution of 1:5000 in 0.5% fat-free milk in phosphate-buffered saline (PBS) containing 0.02% Tween-20 for a primary incubation of 12 h. Horseradish peroxidase-linked secondary antibody (Amersham #NA934) was used at 1:10 000 in PBS/0.02% Tween for a 1 h incubation. Chemiluminescent detection was performed using the ECL kit (Amersham #RPN2106). Immunoprecipitations were performed from 200 μg of pre-cleared total yeast extract with a final dilution of polyclonal antibody of 1:100. The protein A beads were washed extensively including high salt and RIPA buffer washes. For the kinase assay, histone H1 (Sigma #H5505) and [γ-^{32}P]ATP were added in reaction buffer (25 mM MOPS pH 7.2, 5 mM EGTA, 15 mM $MgCl_2$, 60 mM β-glycerophosphate, 0.1 mM Na orthovanadate, 1 mM dithiothreitol, 1 mM phenylmethylsulfonyl fluoride, 2× protease inhibitor cocktail) and the reaction was incubated at 30°C for 30 min. Kinase assays were run on 15 or 10% SDS–PAGE gels, dried and exposed to X-OMAT film for 1–4 h.

Acknowledgements

We are grateful to J.J.Blow, A.M.Carr, J.F.X.Diffley, J.Q.Svejstrup, R.D.Wood and the members of the CDC laboratory for critical reading of this manuscript, and to L.Serrano-Endolz for help with statistical analyses. We thank T.A.Weinert, E.C.Friedberg, M.P.Longhese and M.Foiani for yeast strains. M.A.de la T.-R. is a Marie Curie Fellow supported by EU HC and M Network, contract number CHRX CT94 0685.

References

Aboussekhra,A., Vialard,J.E., Morrison,D.E., de la Torre Ruiz,M.A., Cernakova,L., Fabre,F. and Lowndes,N.F. (1996) A novel role for the budding yeast *RAD9* checkpoint gene in DNA damage-dependent transcription. *EMBO J.*, **15**, 3912–3922.

Allen,J.B., Zhou,Z., Siede,W., Friedberg,E.C. and Elledge,S.J. (1994) The SAD1/RAD53 protein kinase controls multiple checkpoints and DNA damage-induced transcription in yeast. *Genes Dev.*, **8**, 2401–2415.

Baudin,A., Ozier-Kalogeropoulos,O., Denouel,A., Lacroute,F. and Cullin,C. (1993) A simple and efficient method for direct gene deletion in *Saccharomyces cerevisiae*. *Nucleic Acids Res.*, **21**, 3329–3330.

Brunborg,G. and Williamson,D.H. (1978) The relevance of the nuclear division cycle to radiosensitivity in yeast. *Mol. Gen. Genet.*, **162**, 277–286.

Burns,V.W. (1956) X-ray-induced division delay of individual yeast cells. *Radiat. Res.*, **4**, 394–412.

Cohen-Fix,O. and Koshland,D. (1997) The anaphase inhibitor of *Saccharomyces cerevisiae* Pds1 is a target of the DNA damage checkpoint pathway. *Proc. Natl Acad. Sci. USA*, **94**, 14361–14366.

Eckardt Schupp,F., Siede,W. and Game,J.C. (1987) The RAD24 (= Rs1) gene product of *Saccharomyces cerevisiae* participates in two different pathways of DNA repair. *Genetics*, **115**, 83–90.

Elledge,S.J. (1996) Cell cycle checkpoints: preventing an identity crisis. *Science*, **274**, 1664–1672.

Fay,D.S., Sun,Z. and Stern,D.F. (1997) Mutations in *SPK1*/*RAD53* that specifically abolish checkpoint but not growth-related functions. *Curr. Genet.*, **31**, 97–105.

Foreman,P.K. and Davis,R.W. (1994) Cloning vectors for the synthesis of epitope-tagged, truncated and chimeric proteins in *Saccharomyces cerevisiae*. *Gene*, **144**, 63–68.

Friedberg,E.C., Walker,G.C. and Siede,W. (1995) *DNA Repair and Mutagenesis*. ASM Press, Washington, DC.

Hartwell,L.H. and Kastan,M.B. (1994) Cell cycle control and cancer. *Science*, **266**, 1821–1828.

Kim,S. and Weinert,T.A. (1997) Characterization of the checkpoint gene *RAD53*/*MEC2* in *Saccharomyces cerevisiae*. *Yeast*, **13**, 735–745.

Kiser,G.L. and Weinert,T.A. (1996) Distinct roles of yeast *MEC* and *RAD* checkpoint genes in transcriptional induction after DNA damage and implications for function. *Mol. Biol. Cell*, **7**, 703–718.

Longhese,M.P., Fraschini,R., Plevani,P. and Lucchini,G. (1996) Yeast *pip3*/*mec3* mutants fail to delay entry into S phase and to slow DNA replication in response to DNA damage, and they define a functional link between Mec3 and DNA primase. *Mol. Cell. Biol*., **16**, 3235–3244.

Longhese,M.P., Paciotti,V., Fraschini,R., Zaccarini,R., Plevani,P. and Lucchini,G. (1997) The novel DNA damage checkpoint protein Ddc1p is phosphorylated periodically during the cell cycle and in response to DNA damage in budding yeast. *EMBO J*., **16**, 5216–5226.

Lydall,D. and Weinert,T. (1995) Yeast checkpoint genes in DNA damage processing: implications for repair and arrest. *Science*, **270**, 1488–1491.

Morgan,S.E. and Kastan,M.B. (1997) p53 and ATM: cell cycle, cell death, and cancer. *Adv. Cancer Res*., **71**, 1–25.

Murnane,J.P. (1995) Cell cycle regulation in response to DNA damage in mammalian cells: a historical perspective. *Cancer Metastasis Rev.*, **14**, 17–29.

Navas,T.A., Sanchez,Y. and Elledge,S.J. (1996) RAD9 and DNA polymerase epsilon form parallel sensory branches for transducing the DNA damage checkpoint signal in *Saccharomyces cerevisiae*. *Genes Dev.*, **10**, 2632–2643.

Pati,D., Keller,C., Groudine,M. and Plon,S.E. (1997) Reconstitution of a MEC1-independent checkpoint in yeast by expression of a novel human fork head cDNA. *Mol. Cell. Biol*., **17**, 3037–3046.

Paulovich,A.G., Margulies,R.U., Garvik,B.M. and Hartwell,L.H. (1997) RAD9, RAD17, and RAD24 are required for S phase regulation in *Saccharomyces cerevisiae* in response to DNA damage. *Genetics*, **145**, 45–62.

Sanchez,Y., Desany,B.A., Jones,W.J., Liu,Q., Wang,B. and Elledge,S.J. (1996) Regulation of RAD53 by the ATM-like kinases MEC1 and TEL1 in yeast cell cycle checkpoint pathways. *Science*, **271**, 357–360.

Shinagawa,H. (1996) SOS response as an adaptive response to DNA damage in prokaryotes. *EXS*, **77**, 221–235.

Siede,W. and Friedberg,E.C. (1990) Influence of DNA repair deficiencies on the UV sensitivity of yeast cells in different cell cycle stages. *Mutat. Res*., **245**, 287–292.

Siede,W., Friedberg,A.S. and Friedberg,E.C. (1993) RAD9-dependent G_1 arrest defines a second checkpoint for damaged DNA in the cell cycle of *Saccharomyces cerevisiae*. *Proc. Natl Acad. Sci. USA*, **90**, 7985–7989.

Siede,W., Friedberg,A.S., Dianova,I. and Friedberg,E.C. (1994) Characterization of G_1 checkpoint control in the yeast *Saccharomyces cerevisiae* following exposure to DNA-damaging agents. *Genetics*, **138**, 271–281.

Sun,Z., Fay,D.S., Marini,F., Foiani,M. and Stern,D.F. (1996) Spk1/Rad53 is regulated by Mec1-dependent protein phosphorylation in DNA replication and damage checkpoint pathways. *Genes Dev.*, **10**, 395–406.

Walker,G.C. (1984) Mutagenesis and inducible responses to deoxyribonucleic acid damage in *Escherichia coli*. *Microbiol. Rev.*, **48**, 60–93.

Weinert,T.A. and Hartwell,L.H. (1988) The *RAD9* gene controls the cell cycle response to DNA damage in *Saccharomyces cerevisiae*. *Science*, **241**, 317–322.

Weinert,T.A., Kiser,G.L. and Hartwell,L.H. (1994) Mitotic checkpoint genes in budding yeast and the dependence of mitosis on DNA replication and repair. *Genes Dev.*, **8**, 652–665.

Yang,S.S., Yeh,E., Salmon,E.D. and Bloom,K. (1997) Identification of a mid-anaphase checkpoint in budding yeast. *J. Cell Biol*., **136**, 345–354.

Zhou,Z. and Elledge,S.J. (1993) *DUN1* encodes a protein kinase that controls the DNA damage response in yeast. *Cell*, **75**, 1119–1127.

Received December 8, 1997; revised February 20, 1998; accepted March 5, 1998